2023 IEEE/ASME International Conference on Advanced Intelligent Mechatronics (AIM)
June 28-30, 2023. Seattle, Washington, USA

Robot End-effector for Fabric Folding

Akira Seino[1,2], Junya Terayama[3], Fuyuki Tokuda[1,2], Akinari Kobayashi[1,2] and Kazuhiro Kosuge[1,4]

Abstract— **In this paper, we propose a robot end-effector for fabric folding along a straight line for garment production. In the garment production process, some of the edges of fabric parts of a garment need to be folded before sewing. A conventional automated folding system has a fixture designed for each shape and size of the folding part. The fixture is not universal. In the case of a pocket setter, for example, a pocket template of the fixture used for folding needs to be redesigned/reconfigured when the shape of the fabric part changes. A conventional automated fabric folding system is designed for the mass production of garments with the same shape and the same size. In this paper, we consider how to perform fabric folding without the use of a fixture, so that the same system could be used for folding fabric parts of different shapes and sizes. We propose a concept of a robot end-effector for fabric folding along a straight fold line and develop a prototype of an end-effector referred to as"F-FOLD"(Free-form FOLDing). Folding of the edge of a fabric part is achieved by moving F-FOLD along the desired straight fold line. Experimental results illustrate how F-FOLD folds a fabric part along a straight line.**

I. INTRODUCTION

Manufacturing is becoming increasingly automated, with a growing number of industrial robots installed worldwide[1]. The garment industry is one of the manufacturing industries seeking automation. Unlike most industrial parts manipulated by a robot, a fabric part of a garment does not have a stable shape. The shape of the fabric part depends on many factors, such as how it is supported and how forces/moments are applied to it. This makes it very difficult to handle fabric parts with a robot system. Most garment manufacturing processes, including picking and placing, manipulating, folding and sewing fabric pieces, are still done manually.

Automated garment production processes using robots are attracting more and more attention. For example, several research has been carried out on sewing garments [2]–[6], garment folding operations [7]–[9], and end-effectors for garment handling [10]–[12]. Making a garment involves many processes, including cutting, folding and sewing parts of the fabric together. In this paper, we will focus on the folding of fabric edges as one of the processes before sewing. In the production of dress shirts, for example, the sleeves, pockets and collars are folded before they are sewn together.

Fabric folding automation is usually done using a system designed for each fabric part, such as an automatic pocket setter. For example, JUKI Corp. developed an automation system called "pocket setter" for pocket folding and setting [13]. In this system, the fabric part is manually attached to a pocket template designed for folding the pocket, and then a folding mechanism for the pocket folds the edges of the pocket part using the template. Finally, the edge-folded fabric part is placed on the fabric part, to which the pocket is attached, the sewing template is placed on the folded fabric part, and sewing is performed along the grooves of the sewing template. A similar system has also been developed for folding the sleeve placket and placket of shirts [14].

Existing automated systems, including fabric folding, have been designed for the mass production of identical garments. The system designed for a fabric part needs to be modified and reconfigured for a different fabric part with different shapes and dimensions. To solve this problem, we propose a new robot end-effector for fabric folding along arbitrary straight fold lines using a robot manipulator.

Figure 1 illustrates a fabric folding system using the proposed robot end-effector. The system consists of a force and torque sensor (F/T sensor) attached to the endpoint of the manipulator, an end-effector for free form folding (F-FOLD) attached to the F/T sensor, and a suction stage. The suction stage is used to secure the fabric part to the stage during the folding operation. The manipulator moves the F-FOLD along the desired straight fold line with a constant normal force to the stage, based on the information from the F/T sensor, while the suction stage is used to hold the piece of fabric to the table during the folding process.

The remainder of this paper is organized as follows.

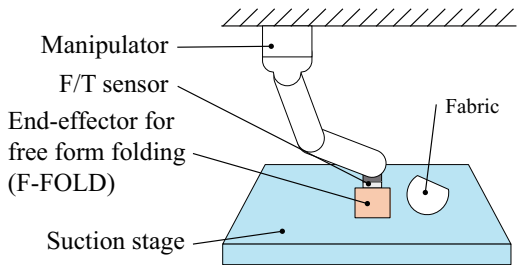

Fig. 1: Fabric folding system using F-FOLD

[1]Akira Seino, Fuyuki Tokuda, Akinari Kobayashi, and Kazuhiro Kosuge are with Centre for Transformative Garment Production, Units 1215 to 1220, 12/F, Building 19W, SPX1, Hong Kong Science Park, Pak Shek Kok, N.T., Hong Kong SAR {akira.seino, fuyuki.tokuda, akinari.kobayashi, kazuhiro.kosuge }@transgp.hk

[2]Akira Seino, Fuyuki Tokuda, and Akinari Kobayashi are with the Department of Electrical and Electronic Engineering, The University of Hong Kong, Hong Kong SAR

[3]Junya Terayama is with Graduate School of Engineering, Tohoku University, 6-6-01 Aoba, Aramaki, Aoba-ku, Sendai, Miyagi 980-8579, Japan j.terayama@srd.mech.tohoku.ac.jp

[4]Kazuhiro Kosuge is Director of the JC STEM Lab of Robotics for Soft Materials, Department of Electrical and Electronic Engineering, Faculty of Engineering, The University of Hong Kong, Hong Kong SAR kosuge@hku.hk

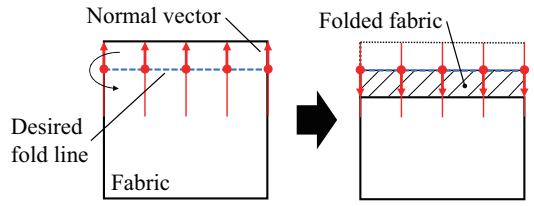

Fig. 2: Folding operation of the edge of the fabric part along a straight line.

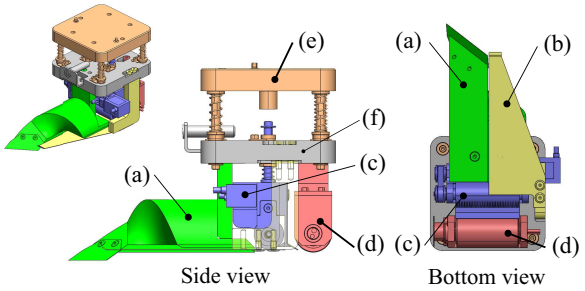

Fig. 3: The design of a prototype of F-FOLD. (a) is the turnover mechanism, (b) is the folding guide, (c) is the fabric feeding mechanism, (d) is the heating iron, (e) is the suspension mechanism, and (f) is the base plate.

Section II introduces the structure of F-FOLD and the folding mechanism of the fabric part. Section III describes the robot control system to fold the fabric part using F-FOLD. Section IV shows the experimental results to illustrate the performance of the proposed end-effector. Finally, Section V concludes this paper.

II. STRUCTURE OF END-EFFECTOR

A. Folding Operation

Let us consider the case where a piece of fabric is placed flat on a horizontal table. As shown in Fig. 2, edge folding means that the normal to the fold line is turned inwards towards the edge of the fabric. For the desired straight fold line, the normal vectors will all be turned inwards and face the same direction after the fold operation has been carried out.

B. Prototype Design

Figure 3 illustrates the structure of a prototype of F-FOLD. F-FOLD consists of a turnover mechanism, a folding guide, a fabric feeding mechanism, a heating iron, and a spring-loaded suspension mechanism attached to the base plate of F-FOLD. The suspension mechanism is used to protect the F/T sensor from the unexpected motion of the robot during the development of the system. The turnover mechanism, the folding guide, and the heating iron are attached to the base plate of the suspension mechanism.

The fabric feeding mechanism is connected to the base plate of the suspension mechanism via another suspension mechanism which consists of linear shafts and slightly pre-compressed springs. The fabric feeding mechanism is used to feed the folded edge of the fabric part to the heating iron.

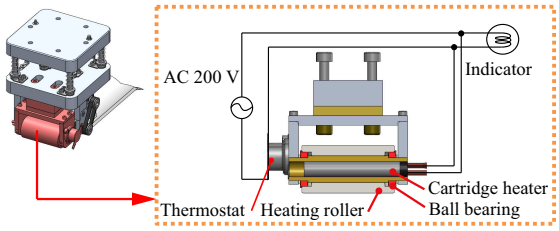

Fig. 4: Structure of the heating iron and the electric circuit to control the temperature of the heating roller.

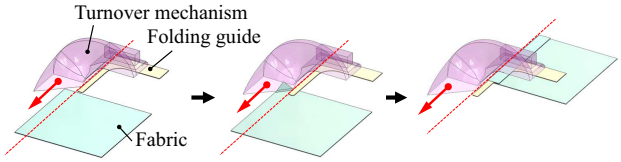

Fig. 5: Folding process 1: turning over the fabric roughly.

The heating iron applies heat and force to the folded edge of the fabric to fix it in place. The structure of the heating iron is shown in Fig. 4. The heating iron is equipped with a cartridge heater, a bimetal thermostat, and a heating roller made of brass.

An electrical circuit is installed to control the temperature of the heating roller using the bimetal thermostat. When voltage is applied, the cartridge heater attached to the roller's rotational shaft heats the heating roller. The thermostat shuts off the circuit when the temperature of the sensing part reaches the operating temperature. When the temperature of the sensing part of the thermostat drops to a certain temperature, the thermostat reconnects the circuit. This process is repeated to maintain the temperature of the iron at an appropriate temperature for folding a cotton fabric. Ball bearings are inserted between the heating roller and the rotating shaft with a built-in cartridge heater, allowing the roller to transmit pressure and temperature to the fabric.

The fabric folding is carried out as follows: When F-FOLD moves along the fold line on the fabric part, F-FOLD roughly turns over the fabric edge using the turnover mechanism and the folding guide as shown in Fig. 5. The turnover mechanism is equipped with an elastic plate at the tip as shown in Fig. 3. When the turnover mechanism starts to move along the fold line, the elastic plate is placed between the fabric part and the suction stage and the folding guide is placed on the fabric part. The fabric feeding mechanism is used to pull the folding edge and align it with the folding guide as shown in Fig. 6.

The rotation of the fabric feeding roller is controlled by a servo motor through the pulley and belt mechanism. When the feed roller rotates, the edge of the roughly flipped fabric is pulled. The flipped fabric rotates around the red point in Fig. 6 and is pressed against the folding guide. The fabric is folded along the edge of the folding guide since the feeding roller pulls the folding edge against the folding guide. The folding edge is fixed using a heating iron attached to the rear end of F-FOLD as shown in Fig. 7.

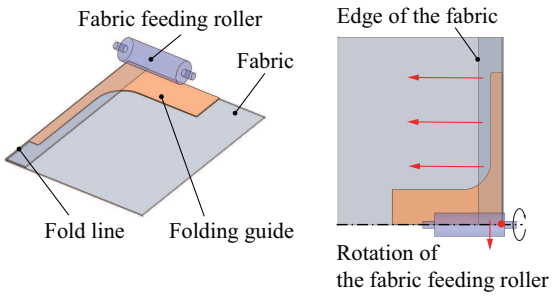

Fig. 6: Folding process 2: folding edge alignment.

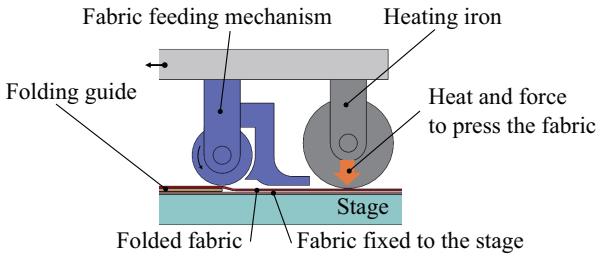

Fig. 7: Folding process 3: folding edge fixing.

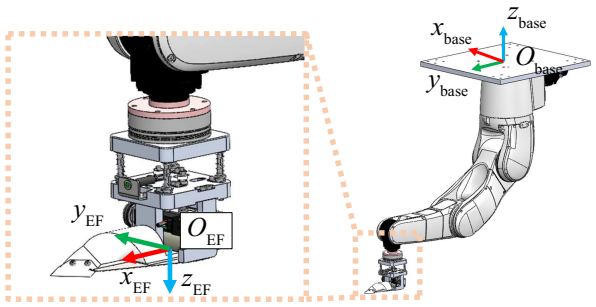

Fig. 8: The coordinate system of the manipulator and F-FOLD.

III. ROBOT CONTROL FOR FOLDING OPERATION

A. Coordinate System of F-FOLD

The end-effector coordinate system $O_{EF}-x_{EF}y_{EF}z_{EF}$ is attached to the bottom of F-FOLD as shown in Fig. 8. The x_{EF} axis coincides with the heading direction of F-FOLD, and the y_{EF} axis coincides with the axial direction of the feeding roller. The z_{EF} axis coincides with the direction of the rotational axis of the final joint of the manipulator.

The desired path is given in the end-effector coordinate system $O_{EF}-x_{EF}y_{EF}z_{EF}$. The manipulator is controlled so that the origin of the end-effector coordinate system follows the desired fold line. For the orientation, the x_{EF}-axis of the end-effector coordinate system is controlled so that it is always tangential to the desired fold line.

B. Impedance Control

An impedance controller is implemented to keep the surface-to-surface contact of F-FOLD with the fabric part [15]. The coordinate system of F-FOLD $O_{EF}-x_{EF}y_{EF}z_{EF}$ is used for the impedance control. xyz Euler angles are used to represent the orientation of the F-FOLD in our system.

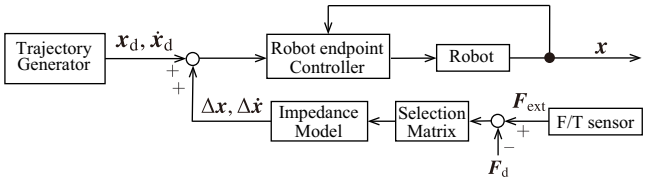

Fig. 9: The block diagram of the hybrid position and impedance controller. $\boldsymbol{x}_d \in \mathbb{R}^6$ and $\dot{\boldsymbol{x}}_d \in \mathbb{R}^6$ are the desired pose and velocity calculated by the trajectory generator. $\boldsymbol{x} \in \mathbb{R}^6$ is the current pose of the end-effector.

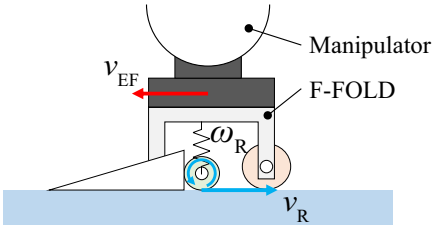

Fig. 10: Relationship between F-FOLD velocity and the angular velocity of the fabric feeding roller.

The block diagram of the control is shown in Fig. 9. The impedance controller controls the apparent impedance of the end-effector. In our case, a hybrid position and impedance controller is designed as follows:

$$\boldsymbol{M}\Delta\ddot{\boldsymbol{x}} + \boldsymbol{D}\Delta\dot{\boldsymbol{x}} + \boldsymbol{K}\Delta\boldsymbol{x} = \boldsymbol{S}(\boldsymbol{F}_{ext} - \boldsymbol{F}_d), \tag{1}$$

where $\boldsymbol{M} \in \mathbb{R}^{6\times6}$ is the apparent inertia matrix, $\boldsymbol{D} \in \mathbb{R}^{6\times6}$ is the apparent damping matrix, and $\boldsymbol{K} \in \mathbb{R}^{6\times6}$ is the apparent stiffness matrix. $\Delta\boldsymbol{x} \in \mathbb{R}^6$ is the displacement from the reference pose calculated by the trajectory generator. $\boldsymbol{F}_{ext} \in \mathbb{R}^6$ is a combination of the three DoF external forces and three DoF external moments acting on the F-FOLD coordinate system. $\boldsymbol{F}_d \in \mathbb{R}^6$ is desired force and torque on the F-FOLD coordinate system. $\boldsymbol{S} \in \mathbb{R}^{6\times6}$ is a selection matrix of position control and force control. This selection matrix $\boldsymbol{S}$ is diagonal, and the diagonal component $\lambda_i, (i = 1,2,\cdots,6)$ are expressed as

$$\lambda_i = \begin{cases} 0 & \text{(for position control)} \\ 1 & \text{(for impedance control)} \end{cases} \quad (i = 1,2,\cdots,6). \tag{2}$$

Equations (1) and (2) allow position and force control to be performed independently for each coordinate.

To make F-FOLD follow the trajectory while pressing the fabric against the stage, position control is applied in the x_{EF} and y_{EF} directions, and damping control in the z_{EF} direction by setting the stiffness coefficient to zero. Impedance control is applied to the rotation around the x_{EF} and y_{EF} axes to keep the surface-to-surface contact of F-FOLD with the fabric part and to press the fabric against the stage.

C. Control of F-FOLD

F-FOLD is equipped with a servo motor for the feeding mechanism, as described in Section III. The fabric feeding mechanism feeds the fabric to the heat roller while the manipulator moves F-FOLD along the desired fold line.

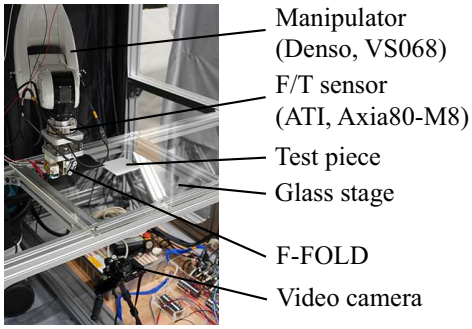

Fig. 11: Experimental system.

TABLE I: Impedance parameters

Parameter	Value
$\boldsymbol{M}$	diag(0.2, 0.2, 0.1, 2, 2, 5)
$\boldsymbol{D}$	diag(1000, 1000, 500, 10000, 10000, 20000)
$\boldsymbol{K}$	diag(2000, 2000, 0, 10000, 10000, 20000)
$\boldsymbol{S}$	diag(0, 0, 1, 1, 1, 0)

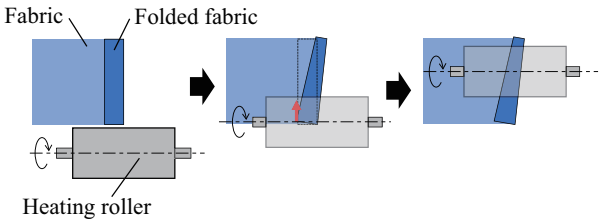

Fig. 12: Misalignment between the fabric on the stage and the folded edge of the fabric occurs when the heating roller rides up on the folded edge of the fabric.

F-FOLD is controlled so that the x_{EF} is always tangential to the desired fold line. Let v_{EF} be the moving velocity of F-FOLD along the x_{EF} direction, ω_{R} be the angular velocity of the feeding roller, and v_{R} the velocity of the feeding roller at the contact point between the feeding roller and the stage. The feeding roller has to rotate so that v_{R} is equal to or larger than v_{EF}. If the angular velocity of the feeding roller is smaller than F-FOLD velocity, the feeding roller will act as resistance, and the fabric will jam in F-FOLD.

Figure 10 illustrates the relationship between the F-FOLD velocity and the angular velocity of the feeding roller. The radius of the roller is defined as r_{R}, and the desired angular velocity of the feeding roller ω_{R} is calculated as

$$\omega_{\mathrm{R}} = -\alpha \frac{v_{\mathrm{EF}}}{r_{\mathrm{R}}}, \tag{3}$$

where α is the velocity ratio of v_{R} to v_{EF} ($\alpha \geqq 1.0$). When $\alpha = 1$, the relative velocity between v_{EF} and v_{R} at the contact point of the feeding roller becomes zero.

IV. EXPERIMENTS

Experiments were conducted to evaluate the basic performance of F-FOLD in the fabric folding operation. In the experiment, the folding operation along a straight line was carried out.

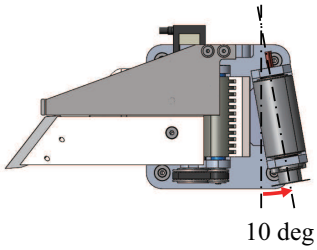

Fig. 13: The heating iron is rotated 10 deg. and placed in F-FOLD.

A. Experimental Setup

As shown in Fig. 11, the experimental system consists of a six DoF manipulator (DENSO: VS068), an F/T sensor (ATI Industrial Automation: Axia80-M8), a concept prototype of F-FOLD, and a transparent stage made of glass. A glass plate is used as a stage instead of the suction stage to observe the F-FOLD folding process.

A camera is placed behind the glass plate to capture the folding process. The fabric is fixed to the plate using double-sided tape during the experiments since the suction stage could not be used to observe the process. The thermostat used for F-FOLD was one with an operating range of 135°C to 160°C. As a servo motor of F-FOLD, an AC servo motor (Yaskawa Electric: Σ-VII SGM7M-B9E3AA1, 11 W) was used. PC (CPU: Intel Xeon W-2255 3.70 GHz, Memory: 64.0 GB) was used to control the manipulator and F-FOLD. Sampling rate of control is 1 kHz. INtime was used for the real-time control system.

B. Method

Figure 15a shows a cotton fabric test piece for the experiment. The fabric size of the test piece is 100 × 100 mm, and desired fold lines are printed at 5, 10, 15, and 20 mm from the edge of the fabric test pieces.

The experimental procedure is as follows:

1) A marker pen attached to the endpoint of the manipulator is controlled to follow a pre-determined desired linear path, and the desired path is drawn on the glass stage.
2) The test piece with the desired fold line drawn on it is placed so that the desired fold line is aligned with the straight line drawn on the stage.
3) F-FOLD is attached to the endpoint of the manipulator, and the manipulator is controlled to follow the same trajectory as that of the marker pen. The hybrid position and impedance controls described in the previous section control the manipulator.

For trajectory generation, a trapezoidal velocity profile is used for the linear path [16]. During the experiments, the desired force of F-FOLD is set to 1.0 N in the z_{EF}-axis direction, and α is set to 1.2. Impedance parameters are determined experimentally as shown in Table I. The folding experiment was performed five times for each fold width.

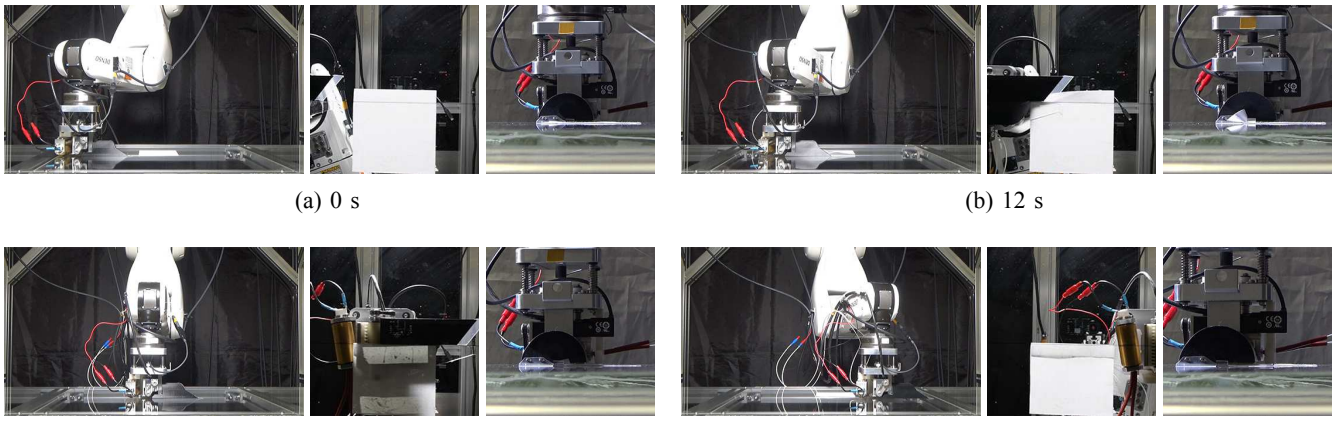

(a) 0 s (b) 12 s

(c) 21 s (d) 32 s

Fig. 14: Fabric folding along the straight line. The left image shows the overall view of the folding operation, the center image is the bottom view captured by the video camera located behind the glass stage, and the right image is the side view of the F-FOLD.

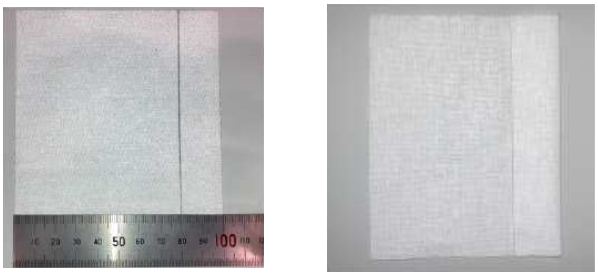

(a) Before folding operation. (b) After folding operation.

Fig. 15: An example of the experimental result before and after folding operation. Fold width is 20 mm.

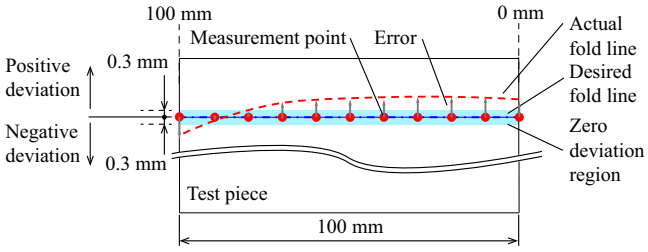

Fig. 16: Position on the fabric where the deviation between the desired fold line and the actual fold line is measured. The thickness of the line drawn by the ballpoint pen is in an area ±0.3 mm from the desired fold line.

C. Results

When the axis of rotation of the heating roller was mounted parallel to the axis of the feeding roller, the folded edge of the fabric deviated from the desired straight line pushed by the heating roller when the heating roller rides up on the fabric, as shown in Fig. 12.

In the following experiment, the heating roller is installed at an angle of 10 deg. as shown in Fig. 13. Figure 14 shows the folding process using the proposed end-effector. As shown in Fig. 14b, the elastic plate of the tip of the turnover mechanism was inserted between the fabric and the stage, the fabric was roughly turned over around the folding guide and aligned with the folding guide by the feeding mechanism. The fabric was fed from the feeding mechanism to the heating iron, and the fold was fixed by the heating iron. As shown in Fig. 14d, the fabric was folded along the desired fold line after F-FOLD finished the folding operation. Figure 15 shows an example of the test pieces after folding with a 20 mm fold width.

TABLE II: The maximum and the minimum average deviations

Fold width (mm)	5	10	15	20
Max. average deviation (mm)	-0.74	0.16	-0.36	-0.32
Min. average deviation (mm)	0.08	0	0	0

In the experiment, F-FOLD was able to fold the fabric along the desired straight fold lines with different widths (5 mm, 10 mm, 15 mm, 20 mm). For evaluating the accuracy of the fold, the deviation between the desired straight line and the actual fold line was measured. The deviation of the fold line from the desired fold line, as shown in Fig. 16, was measured by a calliper. The desired fold lines are drawn with a 0.5 mm thick ballpoint pen. If the actual fold line is on the desired fold line, whose actual width on the fabric was about 0.6 mm, we consider the deviation 0 mm. Note that the measured deviation is from the middle of the desired fold line drawn on the fabric.

Figure 17 shows the average of measured deviations of the actual fold line for each position from the edge. The maximum and the minimum average deviations of each fold width are shown as Table II. These results show that the deviation is larger when the fold width of the fabric is small compared to when the fold width is large.

D. Discussion

By installing the heating iron at an angle, the heating roller exerts a lateral force on the piece of fabric as shown in

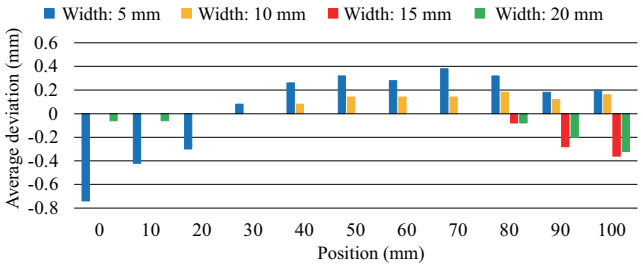

Fig. 17: Average deviation of actual fold line from desired fold line on each measurement position. The error bar represents the standard deviation of the measured deviations. For 10 mm fold width, the deviations at 0 mm to 30 mm are 0 mm. For 15 mm fold width, the deviations at 0 mm to 70 mm are 0 mm. For 20 mm fold width, the deviations at 20 mm to 70 mm are 0 mm.

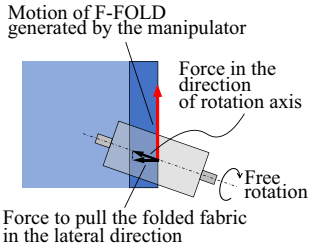

(a) Force generated at the contact point between the fabric and the roller.

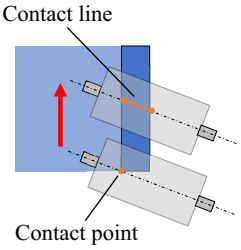

(b) Transition of the contact between the fabric and the roller.

Fig. 18: Effect of placing the heating rollers of F-FOLD at an angle.

Fig. 18a. The resulting lateral force pulls the folded fabric towards the folding guide to align the fold line with the desired fold line indicated by the folding guide. When the fold width is 5mm, the contact line between the fabric and the roller cannot be sufficiently secured and the deviation of the fold line from the desired line was greater than in the other cases. As shown in Fig. 18b, installing the heating iron at an angle also gradually changes the contact area between the heating roller and the fabric section from a point to a line along the roller axis. Folded edge is less likely to be misaligned, even when the folded edge is pushed by the heating roller. This also prevents the folded fabric from deviating from the folding guide.

V. CONCLUSIONS

In this paper, we proposed a robot end-effector, F-FOLD, for the folding of the edge of a fabric part along a straight line for a robot folding system. Without reconfiguring the system, the proposed system can fold a fabric part along a straight line with different fold widths. F-FOLD consists of a turnover mechanism, a folding guide, a fabric feeding mechanism, and a heating iron, attached to the base plate of F-FOLD. Experimental results illustrated how the proposed robot end-effector folds a fabric part along a straight line with different fold widths without the reconfiguration of the system. The proposed system is a concept prototype of the system. Further improvement in folding accuracy and the realisation of free-form folding based on the proposed concept will be presented in the near future.

ACKNOWLEDGMENT

This work was supported in part by the Innovation and Technology Commission of the HKSAR Government under the InnoHK initiative. The research work described in this paper was in part conducted in the JC STEM Lab of Robotics for Soft Materials funded by The Hong Kong Jockey Club Charities Trust.

REFERENCES

[1] IFR presents World Robotics 2022 reports [Online], https://ifr.org/news/wr-report-all-time-high-with-half-a-million-robots-installed (Accessed Jan. 18th, 2023)

[2] G. Biegelbauer, M. Richtsfeld, W. Wohlkinger, M. Vincze and M. Herkt, "Optical Seam Following for Automated Robot Sewing," Proceedings 2007 IEEE International Conference on Robotics and Automation, 2007, pp. 4758-4763, doi: 10.1109/ROBOT.2007.364212.

[3] R. C. Winck, S. Dickerson, W. J. Book and J. D. Huggins, "A novel approach to fabric control for automated sewing," 2009 IEEE/ASME International Conference on Advanced Intelligent Mechatronics, 2009, pp. 53-58, doi: 10.1109/AIM.2009.5230040.

[4] J. Schrimpf and L. E. Wetterwald, "Experiments towards automated sewing with a multi-robot system," 2012 IEEE International Conference on Robotics and Automation, 2012, pp. 5258-5263, doi: 10.1109/ICRA.2012.6224880.

[5] J. Schrimpf, M. Bjerkeng, M. Lind and G. Mathisen, "Model-based feed-forward and setpoint generation in a multi-robot sewing cell," 2015 IEEE International Conference on Robotics and Automation (ICRA), 2015, pp. 2027-2033, doi: 10.1109/ICRA.2015.7139464.

[6] T. Shungo and D. Hisashi, "Development of Fabric Feed Mechanism Using Horizontal Articulated Dual Manipulator for Automated Sewing," 2021 IEEE 17th International Conference on Automation Science and Engineering (CASE), 2021, pp. 1832-1837, doi: 10.1109/CASE49439.2021.9551585.

[7] P. Yang, K. Sasaki, K. Suzuki, K. Kase, S. Sugano and T. Ogata, "Repeatable Folding Task by Humanoid Robot Worker Using Deep Learning," in IEEE Robotics and Automation Letters, vol. 2, no. 2, pp. 397-403, April 2017, doi: 10.1109/LRA.2016.2633383.

[8] A. Doumanoglou et al., "Folding Clothes Autonomously: A Complete Pipeline," in IEEE Transactions on Robotics, vol. 32, no. 6, pp. 1461-1478, Dec. 2016, doi: 10.1109/TRO.2016.2602376.

[9] V. Petrík, V. Smutný and V. Kyrki, "Static Stability of Robotic Fabric Strip Folding," in IEEE/ASME Transactions on Mechatronics, vol. 25, no. 5, pp. 2493-2500, Oct. 2020, doi: 10.1109/TMECH.2020.2980957.

[10] M. T. Kordi, M. Husing and B. Corves, "Development of a multifunctional robot end- effector system for automated manufacture of textile preforms," 2007 IEEE/ASME international conference on advanced intelligent mechatronics, 2007, pp. 1-6, doi: 10.1109/AIM.2007.4412527.

[11] K. Yamazaki and T. Abe, "A Versatile End-Effector for Pick-and-Release of Fabric Parts," in IEEE Robotics and Automation Letters, vol. 6, no. 2, pp. 1431-1438, April 2021, doi: 10.1109/LRA.2021.3057053.

[12] K. M. Digumarti, V. Cacucciolo and H. Shea, "Dexterous textile manipulation using electroadhesive fingers," 2021 IEEE/RSJ International Conference on Intelligent Robots and Systems (IROS), 2021, pp. 6104-6109, doi: 10.1109/IROS51168.2021.9636095.

[13] JUKI Corp. [Online], https://www.juki.co.jp/industrial_e/products_e/apparel_e/automatic_e/detail.php?cd=AP-874S_E (Accessed Feb. 9th, 2022)

[14] M.A.I.C.A. Srl. [Online], https://www.maicaitalia.com/en/product/uam-04/ (Accessed Feb. 9th, 2022)

[15] K. Kosuge, K. Furuta and T. Yokoyama, "Virtual internal model following control of robot arms," Proceedings. 1987 IEEE International Conference on Robotics and Automation, Raleigh, NC, USA, 1987, pp. 1549-1554, doi: 10.1109/ROBOT.1987.1087743.

[16] K. M. Lynch and F. C. Park, Modern Robotics: Mechanics, Planning, and Control. Cambridge University Press, 2017, pp. 331-333.